Interleukin-1α links peripheral $Ca_V2.2$ channel activation to rapid adaptive increases in heat sensitivity in skin

Anne-Mary N Salib[1], Meredith J Crane[2], Sang Hun Lee[3], Brian J Wainger[3], Amanda M Jamieson[2], *Diane Lipscombe[1]

[1]Department of Neuroscience, Carney Institute for Brain Science Brown University, Providence, RI 02912, USA

[2]Department of Molecular Microbiology and Immunology, Brown University, Providence, RI 02912, USA.

[3]Department of Neurology, Harvard Medical School, Massachusetts General Hospital, Boston, MA 02114, USA

*Correspondence: Diane Lipscombe, Carney Institute for Brain Science, Brown University, Providence, RI 02912, USA.

Abstract

Neurons have the unique capacity to adapt output in response to changes in their environment. Within seconds, sensory nerve endings can become hypersensitive to stimuli in response to potentially damaging events. The underlying neuroinflammatory response is well studied, but several of the key signaling molecules that mediate sensory hypersensitivity remain unknown. We previously discovered that peripheral voltage-gated $Ca_V2.2$ channels in nerve endings in skin are essential for the rapid, transient increase in sensitivity to heat, but not to mechanical stimuli, that accompanies intradermal capsaicin. Here we report that the cytokine interleukin-1α

(IL-1α), an alarmin, is necessary and sufficient to trigger rapid heat and mechanical hypersensitivity in skin. Of 20 cytokines screened, only IL-1α was consistently detected in hind paw interstitial fluid in response to intradermal capsaicin and, similar to behavioral sensitivity to heat, IL-1α levels were also dependent on peripheral $Ca_V2.2$ channel activity. Neutralizing IL-1α in skin significantly reduced capsaicin-induced changes in hind paw sensitivity to radiant heat and mechanical stimulation. Intradermal IL-1α enhances behavioral responses to stimuli and, in culture, IL-1α enhances the excitability of *Trpv1*-expressing sensory neurons. Together, our data suggest that IL-1α is the key cytokine that underlies rapid and reversible neuroinflammatory response in skin.

Introduction

Sensory nerve endings in skin are highly plastic; their sensitivity to stimuli can change rapidly, and reversibly, protecting against potentially damaging insults [1]. Neuroinflammatory responses in skin are triggered by intense or high frequency stimulation of peripheral sensory neurons [2]. A critical rise in intracellular calcium in sensory neurons induces the release of inflammatory signaling molecules, including neuropeptides calcitonin gene-related peptide (CGRP), Substance P, and ATP, all of which have downstream consequences on neuroimmune signaling that underlies the cellular changes associated with inflammation and pain [3-7]. The generation of cytokines from immune cell activation via transmitter receptors such as P2X7, is the key step in defining the inflammatory response including its time course and the involvement of different classes of neighboring sensory nerve endings.

The rapid, adaptive increase in sensitivity to sensory stimuli in skin, in response to potentially damaging events, is one of the best-known examples of neuronal adaptation, but the molecules that mediate the initiating, early steps of the neuroinflammatory response are not fully characterized. In an earlier study, we discovered that voltage-gated $Ca_v2.2$ channels expressed in *Trpv1*-nociceptor nerve endings are essential for initiating the rapid neuroinflammatory response to intradermal capsaicin in mice [8]. A highly specific $Ca_v2.2$ channel toxin applied locally in skin inhibited the robust increase in sensitivity to radiant heat that followed intradermal capsaicin. Interestingly, $Ca_v2.2$ channel activity was not essential for the cross-sensitization of mechanoreceptors in the intradermal capsaicin model in the same animals. We also showed that inhibition of P2X7 purinergic receptors, an ATP gated ion channel that activates immune cells to trigger the release of IL-1 inflammatory cytokines [9], reduced intradermal capsaicin-induced rapid heat hypersensitivity in skin [8]. The cytokines that link intense activation of *Trpv1*-

nociceptors to the rapid, early phase of the inflammatory response in skin, notably sensory hypersensitivity of nerve endings across sensory modalities, are incompletely characterized.

Proinflammatory cytokines such as IL-6, IL-1β and TNFα, are generated during neuroinflammatory responses in skin [10-12]. In addition, IL-1β has been shown to induce changes in excitability of neurons in culture, through effects on ion channel currents and second messenger systems [1,13]. These cytokines are elevated in response to prolonged neuroinflammatory conditions associated with pain, however, most studies measure cytokine levels during the later phases of inflammation, not in the initial acute phase of the rapid hypersensitivity response [14,15]. To address this, we extracted and analyzed interstitial fluid from mouse hind paws within 15 mins following intradermal capsaicin, under conditions that result in rapid behavioral changes in skin to sensory stimuli. Intradermal capsaicin is a well-used model of adaptive sensory hypersensitivity in skin with onset and offset kinetics of tens of minutes. This model parallels short-lasting, heat-induced neuroinflammatory responses in human skin [16-18].

We show that IL-1α, a proinflammatory alarmin and one of the earliest immune signaling molecules, is generated locally and abundantly in interstitial fluid in response to intradermal capsaicin. The timing of elevated IL-1α levels parallels peak behavioral hypersensitivity to both radiant heat and mechanical stimuli. Our data suggest that IL-1α is both necessary and sufficient to trigger rapid neuroinflammation in hind paws of both *Trpv1*-noccieptors and mechanoreceptors. Our combined findings suggest that co-activation of TRPV1 receptors and voltage-gated $Ca_v2.2$ channels are necessary to trigger the release of IL-1α that subsequently feeds back on *Trpv1*-nociceptors to enhance heat responsiveness. Understanding the paracrine signaling between sensory nerve endings and immune cells in skin during inflammation will

inform strategies to selectively target maladaptive forms of pain while leaving acute pain relatively intact.

Results

Intradermal capsaicin injection induces a robust, rapid, and reversible increase in the sensitivity of the paw to both heat and mechanical stimuli. To identify the cytokines released in the hind paw in response to intradermal capsaicin, and to assess the dependency of cytokine release on peripheral $Ca_V2.2$ channel activity, we recovered 7-10 µl of interstitial fluid from both paws of each animal, 15 min post injection of capsaicin using three experimental conditions: Intradermal capsaicin in WT, in global $Ca_V2.2^{-/-}$ KO, and in WT co-injected with ω-CgTx MVIIA. At the 15 min time point, after capsaicin injection, behavioral responses to radiant heat and mechanical stimuli were enhanced significantly ([8]; Fig. 2). The $Ca_V2.2^{-/-}$ KO mouse strain was generated in our lab and is a global deletion of $Ca_V2.2$ (as described previously [8]). ω-CgTx MIIA is a high affinity, selective, and slowly reversible inhibitor of voltage-gated $Ca_V2.2$ channels [19,20]. We co-injected ω-CgTx MIIA together with capsaicin to assess the contributions of peripheral voltage-gated $Ca_V2.2$ channels in the skin, at the site of injection [8,21,22].

IL-1α levels are elevated in interstitial fluid in hind paws in response to intradermal capsaicin

Pilot screens of 20 cytokines were performed on hind paw fluid samples from each experimental condition between two immunoassays, a multiplex bead-based immunoassay (LEGENDplex) and an electrochemiluminescence spot-based immunoassay (MSD, see Methods). Based on these results, and reports in the literature, 13 cytokines were selected as likely neuroinflammatory candidates and screened for using a custom mouse panel LEGENDplex panel. Pooled, paw fluid samples (n = 11-22 mice) were screened. Of the 13 cytokines assayed, only IL-1α was consistently detected in hind paw fluid under any condition at the 15

min time point. We used a second independent custom panel, Meso Scale Discovery (MSD), to validate IL-1α levels in the same samples. In addition, we assessed: 8 of the same 13 cytokines surveyed on the LEGENDplex, as well as 3 cytokines that were undetectable on our pilot LEGENDplex screen, and macrophage derived chemokine (MDC) which was unique to the MSD platform (Fig. 1a).

IL-1α levels were increased significantly in response to intradermal capsaicin in WT mice as compared to saline injected paws (capsaicin vs saline; two-way ANOVA with Tukey correction: $p=0.0002$; Fig. 1b). The IL-1α response to capsaicin was reduced in $Ca_V2.2^{-/-}$ global KO mice (Fig. 1b; $p=0.0158$) and also in WT mice co-injected with ω-CgTx MVIIA (Fig. 1b; $p=0.0025$), as compared to samples from WT hind paws. We compared the IL-1α levels in hind paws of capsaicin-injected $Ca_V2.2^{-/-}$ and WT mice co-injected with ω-CgTx MVIIA mice and these were similar to levels in control hind paws injected with saline (Fig. 1b).

To control for the possible involvement of systemic differences in IL-1α levels across mice under different experimental conditions, we measured IL-1α in serum of the same experimental animals. IL-1α levels in serum were much lower than those at the site of capsaicin injection and they were unaffected by intradermal capsaicin (Fig. 1c). We consistently detected low levels of two cytokines in addition to IL-1α in serum samples, CXCL10 and CCL5, and the levels of these cytokines were not correlated with intradermal capsaicin injection.

As a complementary approach to measuring cytokines in interstitial fluid using the LEGENDplex and MSD platform, we used a single analyte ELISA to measure IL-1α levels in hind paw skin-conditioned media. Skin from hind paws of WT mice injected intradermally with capsaicin (ipsilateral) and saline (contralateral) were harvested 5 mins post injection. IL-1α levels in hind paw skin-conditioned media from capsaicin injected paws were significantly higher, as

compared to those from saline injected hind paws (5 of 6 mice; Fig. 1d; $p = 0.01$, paired t-test). Collectively, our data show that intradermal capsaicin triggers IL-1α release in hind paws within the first 5 mins of injection, paralleling the rapid time course of behavioral changes in hind paw sensitivities to heat and mechanical stimuli ([8]; Fig. 2).

IL-1α is necessary for the development of capsaicin-induced increases in sensitivity to heat and mechanical stimuli

To establish if IL-1α levels are increased *and* necessary for capsaicin-induced changes in hind paw sensitivity to heat, we co-injected a specific neutralizing monoclonal IL-1α antibody (anti-mIL-1α-IgG, InvivoGen, Catalog # mabg-mil1a) to occlude its actions locally, at the same site of capsaicin injection. We measured hind paw sensitivity to radiant heat and to mechanical stimuli in WT mice following capsaicin injection in the absence, and in the presence of anti-mIL-1α-IgG (Fig. 2). Baseline behavioral responses to heat and mechanical stimuli were not consistently affected by anti-mIL-1α-IgG ruling out any direct effect on stimulus-response pathways. By contrast, anti-mIL-1α-IgG reduced significantly capsaicin-induced increases in the sensitivity of mouse hind paws to both heat ($p = 0.008$) and to mechanical ($p = 0.012$) stimuli (Fig. 2a, 2b). These data point to a critical role for IL-1α in mediating local and rapid signaling between neurons and immune cells, underlying the capsaicin-induced neuroinflammatory response in skin. Neutralizing IL-1α locally, at the site of capsaicin injection, almost completely attenuated the hypersensitivity response that invariably develops within minutes of intradermal capsaicin.

To establish if IL-1α is sufficient to induce rapid changes in the sensitivity of skin to heat and mechanical stimuli, we directly injected recombinant IL-1α (R&D catalog #: 400-ML-005/CF) into the hind paws of mice and assessed their behavior. Paw withdrawal responses to both heat and mechanical stimuli were evoked with shorter latencies (heat) and at lower forces (mechanical) in

mice injected with recombinant IL-1α at 15- and 30-min time points post injection, as compared to responses of contralateral paws in the same animals (Fig. 3). Similarly, recombinant IL-1α injected paws were hypersensitive to radiant heat and mechanical stimuli as compared to vehicle injected controls (PBS 10% FBS); Heat: 15 mins rIL-1α compared to vehicle $p = 0.07$, mechanical at 15 min $p = 0.02$. Heat: 15 mins rIL-1α compared to vehicle $p = 0.07$, mechanical at 15 min $p = 0.02$. Heat: 30 mins rIL-1α compared to vehicle $p = 0.005$, mechanical at 30 min $p = 0.056$.

Based on our findings, we conclude that IL-1α is a critical early mediator of transient heat and mechanical hypersensitivity in skin induced by capsaicin. Notably, IL-1α was the only cytokine consistently detected in two different cytokine detection platforms used in our analyses. Our data also show that IL-1α levels are strongly dependent on both TRPV1 receptor activation and peripheral $Ca_V2.2$ channel activity, suggesting that IL-1α is a key immune signal underlying the rapid and robust neuroimmune response in skin to heat. Interestingly, even though capsaicin-induced hypersensitivity to mechanical stimulation is independent of $Ca_V2.2$ channel activity [8], we show here that it does depend on IL-1α.

Overnight incubation of IL-1α increases excitability of sensory neurons

To evaluate the impact of IL-1α on nociceptor excitability of primary sensory neurons, we employed APPOINT (Automated Physiological Phenotyping of Individual Neuronal Types), a high-content calcium imaging platform integrating high-throughput single-cell calcium imaging, liquid handling, automated cell segmentation, and analysis [23]. We isolated dorsal root ganglia (DRG) neurons from mice expressing light-sensitive ion channel channel-rhodopsin (ChR2) in *Trpv1*-nociceptors and identified optically responsive neurons using a red-shifted calcium indicator for threshold screening. Compared to vehicle-treated control cells, cells incubated overnight with IL-1α (100 ng/ml) were more responsive to optical stimulation (Fig. 4a), based on

a significant increase in the percentage of calcium-responsive cells (Fig. 4b; $F_{1,40} = 4.27$; $P = 0.045$, two-way ANOVA). These data show that IL-1α can act directly on sensory neurons to alter neuronal excitability via the Interleukin-1 receptor type 1 **(**IL-1R1) receptor on sensory neurons, as has been shown previously for IL-1β [13].

Discussion

Intradermal capsaicin is used to model one of the most well-known examples of the rapid neuroinflammatory response in skin following exposure to potentially damaging stimuli [16,24,25]. We applied this model in mouse hind paw to analyze rapidly generated cytokines in interstitial fluid *in vivo* and, under the same experimental conditions, to monitor behavioral responses to radiant heat and mechanical stimulation. By two independent assays, we identified IL-1α as the major cytokine generated in hind paw fluid, and showed it was both necessary and sufficient to support the rapid increase in sensitivity of peripheral nerve endings in skin to sensory stimuli.

Somewhat surprisingly, IL-1α was the only cytokine consistently present in mouse hind paw fluid and its levels were elevated within 15 mins of intradermal capsaicin exposure, coincident with robust behavioral changes to both radiant heat and mechanical stimuli. Levels of IL-1α measured in hind paw interstitial fluid were 3-4 fold higher following capsaicin injection in WT fluid, when compared to the dynamic range of IL-1α found in blood in non-injured states [26]. We did not detect other inflammatory cytokines in interstitial fluid samples at the 15 min time point; when behavioral responses are maximal. Importantly, in both assays we confirmed that IL-6, IL-1β,and TNFα and all other cytokines included in the screen, were detectable in concurrently run standards (Supplementary File S2).

Our data are consistent with the known role of IL-1α, an alarmin, as one of the earliest signaling molecules of the inflammatory response [27]. In fluid samples of human blisters, IL-1α, not IL-1β, levels are elevated [28,29]. IL-1α is primed and ready in skin resident immune cells for rapid action and, unlike IL-1β which is only biologically active in its cleaved mature form [30-32], IL-1α activates IL-1R1 in both its cleaved mature and precursor pro forms [30]. The known kinetics of IL-1α are faster than IL-1β following stimulation. Others have shown that on the timescale of hours, IL-1α is maximal within 6 hours of stimulation, while IL-1β is maximal 12-16 hours after stimulation [33].

We took a number of steps to validate our findings including: i) Employing two independent cytokine detection platforms, Custom Mouse Panel LEGENDplex and Meso Scale Discovery, designed to identify low levels of cytokines in low volume fluid samples; ii) Screening 20 different cytokines; iii) Using single analyte ELISA to measure IL-1α in isolated skin conditioned media; and iv) Using standards to ensure that the cytokine assays are able to detect all cytokines screened, including IL-1β (Supplementary File S2).

To establish if IL-1α is necessary for the rapid behavioral changes in sensitivity to sensory stimuli associated with intradermal capsaicin, we employed a potent neutralizing antibody anti-mIL-1α-IgG. Anti-mIL-1α-IgG is selective for IL-1α, and it inhibits the biological activity of both precursor and mature forms of mouse IL-1α (InvivoGen, Catalog # mabg-mil1a). By contrast, pharmacological inhibition of the IL-1R1 does not distinguish between IL-1α and IL-1β as both cytokines act through the same receptor [30,34,35]. The almost complete neutralization of the effects of intradermal capsaicin by anti-mIL-1α-IgG, combined with the demonstration that intradermal recombinant IL-1α induces heat and mechanical hypersensitivity in mouse hind paw, establish IL-1α as an immune signal that mediates the rapid increase in peripheral nerve ending sensitivity to heat and mechanical stimulation.

In this study we focus on identifying the cytokine in hind paw that underlies the rapidly developing, and rapidly reversible neuroinflammatory response in skin. Many other cytokines including IL-6, IL-1β, and TNFα are critical for mediating more sustained forms of inflammation associated with chronic pain [2,10-12]. It is possible that IL-1α has been overlooked as critical for the rapid early phase of neuroinflammation in skin because of the focus on chronic inflammatory models of pain, important for identifying new therapeutic targets [36-38], and the use of assays that do not distinguish IL-1α and IL-1β.

We showed previously that voltage-gated $Ca_V2.2$ channels in peripheral nerve endings in skin play a critical role in the development of capsaicin-induced hypersensitivity to heat [8]. Here we show that $Ca_V2.2$ channel activity also mediates the levels of IL-1α in hind paw fluid in response to intradermal capsaicin. Our data are consistent with a model in which voltage-gated $Ca_V2.2$ channels in *Trpv1*-noccieptor nerve endings and IL-1α generating immune cells function as a signaling unit mediating rapid neuroinflammatory responses (Fig. 5). Our data lend support to previous studies showing that $Ca_V2.2$ channels (N-type) are involved in inflammatory and neuropathic pain responses, as well as in microglial activation and cytokine release [39,40]. It is possible that different classes of voltage gated calcium channels contribute to the generation of IL-1α via mechanoreceptor activation. For example, $Ca_V3.2$ channels (T-type), are abundant in low threshold mechanoreceptors (LTMRs) [41] and they have been implicated in neuroinflammatory pain signaling underlying mechanical allodynia [42-44] .

The cross-sensitization of peripheral nerve endings in skin following intradermal capsaicin or naturalistic stimuli is a classic feature of the rapid protective neuroinflammatory response [16,18,45-47]. Our findings, using the intradermal capsaicin model of rapid inflammation, suggest that IL-1α

may also recruit different sensory modalities beyond the target nerve endings of the initiating stimulus [16,48]. We know from our earlier studies, that capsaicin-induced mechanical hypersensitivity develops independent of peripheral $Ca_V2.2$ channel activity in *Trpv1*-nociceptors in the same skin regions [8]. But, anti-mIL-1α-IgG occludes both heat and mechanical hypersensitivity induced by capsaicin (Fig 2c, 2d), suggesting that sufficient IL-1α must be generated, independent of $Ca_V2.2$ channel activity, to act on LTMR nerve endings in skin. Expression levels of IL-1R1 are higher in LTMRs and proprioceptors as compared to *Trpv1*-expressing neurons [41] therefore, it is also possible that *Trpv1*-nociceptors and LTMRs respond to different levels of IL-1α.

Others have shown that IL-1R1 receptor activation by IL-1β increases the excitability of cultured neurons isolated from DRG, including via actions on voltage-gated sodium ion channels and potassium channels [13,43,49-51]. As IL-1α acts through the same IL-1R1 receptor as IL-1β, IL-1α should have similar biological effects [27,30,32,34]). We confirmed this using calcium imaging and optogenetic stimulation of *Trpv1*-nociceptors. In this platform we show that overnight incubation of IL-1α increases the excitability of cultured *Trpv1*-nociceptors compared to control (Fig. 4a., Fig. 4b.), consistent with other reports using similar methods to assess the actions of proinflammatory cytokines on sensory neurons *ex vivo* [52]. Additional studies will be needed to compare the effects of IL-1α on *Trpv1*-nociceptors and LTMR mechanoreceptors that innervate hind paw [48,53-55].

In conclusion, we report that IL-1α is the critical cytokine released from immune cells in skin, underlying rapid, transient, and adaptive neuroinflammation in skin induced by intradermal capsaicin. IL-1α is necessary and sufficient to couple intense stimulation of *Trpv1* nociceptors to a rapidly developing, but transient, hypersensitivity of local nerve endings in skin to heat and mechanical stimuli. IL-1α participates in cross-sensitization of neighboring mechanoreceptor nerve endings.

The *in vivo* actions and time course of IL-1α levels in skin, parallel the behavioral responses that define rapid, adaptive neuroinflammation. Our studies provide important insight for the development of more precise therapeutic strategies to target specific phases of the neuroinflammatory response.

Materials and Methods

All mice used were bred at Brown University, and all protocols and procedures were approved by the Brown University Institutional Animal Care and Use Committee (IACUC). All experiments were performed in accordance with approved IACUC protocols and compliance with ARRIVE guidelines. Male and female mice were included in all experiments and were 3-6 months old, unless otherwise specified. Values shown are mean ± SE. Experimenters were blind to animal genotype, experimental condition, and solution injected and were only unblinded post analysis, including analysis of interstitial fluid. The $Ca_V2.2^{-/-}$ global deletion (KO) mouse strain (*Cacna1b*$^{tm5.1DiLi}$, MGI) was generated in our lab by STOP cassette in frame, in exon 1 of *Cacna1b,* as described previously [8]. A wild-type strain was bred in parallel from the same genetic background and used for comparison in some experiments. These wild-type mice were not significantly different in behavioral studies from wild-type littermates and were pooled for analysis.

Hind paw fluid extraction

Mice were anesthetized using isoflurane (2.0-3.5%) and O_2 (0.6-0.8 LPM) administered continuously via nose-cone for the entire fluid extraction process. The plantar surface of the footpad was injected with 30 gauge insulin needle intradermally in the center of the paw with 50 µl of: 0.1% w/v capsaicin, 0.1% w/v capsaicin + 2 µM ω-conotoxin MVIIA, or 2 µM ω-conotoxin MVIIA using saline as vehicle in all solutions. For fluid extraction, the same syringe is used to optimize yield. Fluid is collected by slowly drawing back the syringe to pull any free fluid in the subcutaneous pocket. Light pressure is applied to the surrounding area and any leaked fluid on the surface was collected. Typical fluid yield is 7-10 µl from two paws per animal and samples from 2-4 animals for each condition are pooled into a Eppendorf on dry ice and stored at -80°C until used for immunoassay analyses.

Serum isolation

Blood was collected postmortem from the heart via cardiac puncture, samples were pooled from the same animals as their corresponding hind paw fluid samples, and after a 45 min coagulation step, centrifuged at 4°C for 12 min at 4000 RPM. Serum supernatant was stored at -80°C for subsequent immunoassays.

Immunoassays

Multiplex bead-based immunoassay (LEGENDplex) fluid analyses: Custom Mouse Inflammation Panel LEGENDplex (BioLegend, LEGENDplex™) protocol was followed according to manufacturer's recommendations and data was acquired using an Attune NxT Flow Cytometer. Pilot hind paw fluid samples from all experimental conditions were collected and used to determine sample dilution factors and to screen for 19 cytokines using capture beads targeting: GM-CSF, IL-1α, IL-1β, IL-4, IL-6, IL-9, IL-10, IL-12p70, IL-17A, IL-22, IL-23, IL-33, TNF-α, IFN-γ, CCL2, CXCL10, CCL4, CCL5, and LIF. We only detected IL-1α in hind paw fluid in the capsaicin model. After initial screening we selected 13 cytokines for ongoing analyses based on consistent detection in pilot studies and on published literature indicating potential role in neuroinflammation in skin. Biolegend LEGENDplex Data Analysis Software Suite (Qognit) was used to determine analyte mean fluorescence intensities and calculate concentrations based on concurrently-run standard curves (Supplementary File S1).

Electrochemiluminescence spot-based immunoassay fluid validation: Following LEGENDplex analyses, remaining samples were assayed on two custom Meso Scale Discovery biomarker panels (MSD R-plex: IL-1α, IL-6; U-plex: TNFα, IL-1β, CCL2, CCL4, CXCL-10, IFNγ, IL-33, IL-10, Il-23, MDC). All samples underwent the same freeze thaw frequency and duration

cycles. MSD Biomarker Group 1 (Mouse) protocol was followed according to the manufacturer's recommendations for 96 well plate assays. Plates were read and analyzed using an MESO QuickPlex SQ 120MM instrument. Final concentrations reported were adjusted for sample dilution. The concentration of a particular cytokine was determined using a calibrator standard assayed on each plate.

Skin explant conditioned media preparation: In anesthetized mice (n=6), we injected capsaicin in one paw, and saline in the contralateral paw prior to skin removal. Mice were euthanized 5 mins post injection and skin was removed from hind paws using 3.5 mm punch biopsy tools (MedBlade, 2 punches/paw). Skin from saline injected-contralateral and capsaicin injected-ipsilateral paws were incubated separately in 600 µl of prewarmed 37°C RPMI 1610 culture media in 12 well plates. Samples were agitated for 5 min at 250 RPM on an orbital shaker, then 200 µl of conditioned media removed for analysis. Conditioned media was run in duplicate using an IL-1α ELISA (ELISA MAX Deluxe Set Mouse IL-1α, BioLegend catalog # 433404).

Behavioral assessments: Radiant heat responses were assessed using Hargreaves (Plantar Analgesia Meter IITC Life Science). Mice were placed in Plexiglas boxes on an elevated glass plate and allowed to habituate for 30 min prior to testing. A radiant heat source was positioned beneath the mice and aimed using low-intensity visible light to the plantar surface of the hind paw. For all trials, laser settings were: Idle intensity at 5% and active intensity at 50% of maximum. Cut off time = 30 s. Trials began once the high-intensity light source was activated and ended once the mouse withdrew, shook, and/or licked their hind paw following stimulation. Immediately upon meeting response criteria, the high-intensity light-source was turned off. The response latency was measured to the nearest 0.01 s for each trial using the built-in timer corresponding to the duration of the high-intensity beam. Three trials were conducted on each

hind paw for each mouse, with at least 1 minute rest between trials [56]. The average of 3 trials was used for the analysis. N values reported are the number of mice.

Mechanical responses were elicited by an automated Von Frey Plantar Aesthesiometer (catalog #37550, Ugo Basile). Mice were placed in an elevated Plexiglas box with a wire mesh bottom and were allowed to habituate for 30 min prior to testing. The plantar surface of hind paws was assessed using a steady ramp of force ranging from 0 to 8g for up to 90 sec. The trial is automatically terminated when the filament buckles or the paw is withdrawn, force and reaction time are captured.

Primary DRG harvesting and culture: For optogenetic calcium imaging experiments, male and female mice (C57Bl6/J) between 14-21 days old were used. *Trpv1*/*ChR2-EYFP* strains were generated by crossing *Trpv1-Cre* (Jax 017769) male mice with LSL-*ChR2-EYFP* (Jax 024109) female mice. C1-L6 dorsal root ganglia (DRG) were dissected from isolated and bisected spinal columns of postmortem mice. DRG were placed in cold DMEM/F-12 media (Thermo Fisher 11320033), and transferred to collagenase/dispase for 60 minutes at 37°C. To dissociate cells, a series of mechanical trituration steps were performed. Cells were filtered through a strainer, centrifuged using a BSA gradient to separate out debris, and plated on a poly-D-lysine (PDL)/laminin treated 96-well plate. All primary sensory neurons were imaged after being cultured overnight in neurobasal media (Thermo Fisher 211 03049) supplemented with B27 (Thermo Fisher 17504044), Glutamax (Thermo Fisher 35050061), and Penicillin-Streptomycin (Thermo Fisher 15070063).

Calcium imaging assay: Calcium imaging experiments were performed using an ImageXPress micro confocal high content imaging system (Molecular Devices). Cells were incubated with CalBryte-630AM (AAT Bioquest 20720, 3 µg/mL in 0.3% DMSO) calcium indicator for 30

minutes in the dark. Media was then replaced with 100 µL physiological saline (in mM: 140 NaCl, 5 KCl, 2 $CaCl_2$, 1 $MgCl_2$, 10 D-glucose, 10 HEPES and pH 7.3-7.4 with NaOH) immediately prior to cell imaging. For optogenetics experiments, three trains of blue light pulses (1, 5, 10 pulses per train; 1 ms each at 50 Hz) were delivered and cells were imaged using the APPOINT calcium imaging assay, as described previously [23].

Data quantification and statistical analysis: Initial identification and quantification of CalBryte-630AM intensity was performed using a custom journal in ImageXPress (Molecular Devices) analysis software. Briefly, CalBryte-positive cells in each well were identified using a minimum projection of the timelapse image stack based on size and CalBryte intensity. Each cell automatically generated an individual ROI, which was transferred back to the original timelapse stack and the mean intensity of each ROI was calculated for every image. Analysis of cell intensity and quantification was performed in R (Version 4.3.1). Statistical analyses were performed using RStudio (Posit Software), Prism (Version 10; GraphPad) or Excel (Microsoft). All data are presented as the mean ± SE. The significance of optical rheobase assay was assessed using two-way ANOVA followed up by Bonferroni's multiple comparisons.

Data Availability Statement

The $Ca_V2.2^{-/-}$ mouse strain ($Cacna1b^{tm5.1DiLi}$) is described in the MGI database and available by request to Diane Lipscombe. All datasets are available by request to Diane Lipscombe.

Competing interests

DL is a member of the Scientific Advisory Board of Zymedyne Therapeutics, Calgary, Canada.

Author contributions

A-M.N.S, M.J.C, S.H.L, B.J.W, A.M.J and D.L. contributed to research design; A-M.N.S, M.J.C, and S.H.L performed research experiments; A-M.N.S, M.J.C, S.H.L, and D.L. analyzed data; A-M.N.S and D.L wrote the paper.

Figure Legends

Figure 1. The cytokine IL-1α is present in paw interstitial fluid and its levels increase with intradermal capsaicin and local $Ca_V2.2$ channel activity. **a.** Experimental procedures and cytokines screened are shown. Interstitial fluid extracted 15 mins following 50 µl intradermal injection in both paws of 0.1% w/v capsaicin, saline, 0.1% w/v capsaicin with 2 µM ω-conotoxin MVIIA, or saline with 2 µM ω-conotoxin MVIIA. Pooled samples were screened for 20 cytokines listed. **b.** IL-1α levels in hind paw fluid based on panel standards, detected using an inflammatory multiplex bead-based immunoassay (BioLegend, Legendplex). Individual points represent pooled samples from wild-type (WT, gray), $Ca_V2.2^{-/-}$ (KO, red), and WT co-injected with ω-conotoxin MVIIA (CgTx-MVIIA, blue). Number of (pooled samples/mice) for WT with saline (7/18); KO with saline (5/11); WT with capsaicin (7/20); KO with saline (7/17); WT with capsaicin + CgTx-MVIIA (5/14); WT saline with CgTx-MVIIA (4/12). Mean ± SE for capsaicin: WT = 1159 ± 272 pg/ml; KO = 561 ± 117 pg/ml; WT + CgTx MVIIA = 343 ± 83 pg/ml. p-values calculated by two-way ANOVA with Tukey HSD correction for multiple comparisons hind paw fluid WT capsaicin|WT saline: p=0.0002; KO capsaicin|KO saline: p=0.1600; WT CgTx-MVIIA + capsaicin|WT CgTX-MVIIA + saline: p= 0.4732. WT capsaicin| KO capsaicin: p = 0.0158; WT capsaicin|WT CgTX-MVIIA + capsaicin: p=0.0025;KO capsaicin|WT CgTX-MVIIA + capsaicin: p=0.5875. **c.** IL-1α levels in serum detected using the same cytokine screening protocol as in Fig 1b. Individual points represent pooled samples from the same animals used for hind paw fluid analysis. Analysis of variance interaction between Injection|Genotype was measured by two-way ANOVA: p=0.8422. **d**. IL-1α levels in skin-explant conditioned media detected using a single analyte ELISA (n=6). Skin punch biopsies were removed 5 mins post-injection and placed in media for 5 mins. Each mouse was injected with saline in one paw and capsaicin in the other for within animal comparison. Average skin weight for capsaicin injected skin: 5.48 mg; saline injected skin: 4.82 mg. Points represent analysis of conditioned media from each paw and solid

lines connect saline and capsaicin injected paws for each mouse; p-value calculated by paired t-test: p= 0.0099.

Figure 2 Neutralizing IL-1α in the presence of capsaicin reduces both heat and mechanical hypersensitivity**.** Paw withdrawal response latencies to radiant heat (**a, b**) and mechanical force (g) using automated Von Frey filament (**c, d**) represented as mean values (lines) ± SE (shaded area) (*left*; **a,c**) and average responses for individual mice (solid circles) and average values for all mice (horizontal line) represented as percent change from baseline (0 mins) (*right*; **b, d**). Measurements were made immediately prior to (0), and 15 and 30 mins post intradermal (*id*) injections as noted. **a, b.** WT ($Ca_V2.2^{+/+}$) mice received 20 µL *id* of: 1 µg/ml Anti-mIL-1α-IgG (orange; n=8); 0.1% w/v capsaicin + 1 µg/ml Anti-mIL-1α-IgG (blue; n=9); 0.1% w/v capsaicin (red; n=8). Mean ± SE latencies to heat at 15 mins: 1 µg/ml Anti-mIL-1α-IgG = 17.7 ± 1.6 s; 0.1% w/v capsaicin + 1 µg/ml Anti-mIL-1α-IgG = 13.3 ± 1.5 s; 0.1% w/v capsaicin = 5.6 ± 0.6 s. **b.** 15 min post: capsaicin + 1 µg/ml Anti-mIL-1α-IgG (blue) = -8.35 ± 12.97%; capsaicin (red) = -59.08 ± 4.84%; Anti- mIL-1α-IgG (orange) = 0.88 ± 9.58%. Type | Time interaction p = 0.0008; at 15 min post *id* for: Capsaicin + 1 µg/ml Anti-mIL-1α-IgG | Capsaicin: p=0.0001; Capsaicin + Anti-mIL-1α-IgG | Anti- mIL-1α-IgG p= 0.6887. **c.** 1 µg/ml Anti-mIL-1α-IgG (orange, n = 7); 0.1% w/v capsaicin + 1 µg/ml Anti-mIL-1α-IgG (blue, n = 7); 0.1% w/v capsaicin (red, n = 7). Mean ± SE values were 1 µg/ml Anti-mIL-1α-IgG = 4.09 ± 0.13 g; 0.1% w/v capsaicin + 1 µg/ml Anti-mIL-1α-IgG = 3.59 ± 0.49 g; 0.1% w/v capsaicin = 2.10 ± 0.24 g. **d.** 15 min post: capsaicin + ml Anti-mIL-1α-IgG (blue) = -21.23 ±13.00%; capsaicin (red) = -52.40 ± 6.04%, 1 µg/ml Anti- mIL-1α-IgG (orange) = -15.90 ± 4.36%. Injection Type| Time interaction: p = 0.0101; 15 min post *id* for: capsaicin + 1 µg/ml Anti-mIL-1α-IgG | Capsaicin: p = 0.0179; capsaicin + Anti-mIL-1α-IgG | Anti- mIL-1α-IgG p = 0.8753. Analysis of variance measured by two-way ANOVA and Tukey's HSD correction for multiple comparisons.

Figure 3 Intradermal recombinant IL-1α triggers both heat and mechanical hypersensitivity in the absence of capsaicin **a**. Response latency (s) to radiant heat measured before (0) and 15 and 30 mins after 20 µg/ml injection of 5 µg/ml recombinant mouse IL-1α (m-IL-1α) in sterile PBS + 10% FBS (n = 6). Injected (red) and un-injected paws (blue). Mean ± SE response latencies to heat 15 mins following injection to: m-IL-1α: 9.66 ± 1.26 s and un-injected 16.06 ± 1.84 s. **b**. Percentage change from baseline for Individual mice in response to m-IL-1a (15 min) -31.03 ± 6.36% and un-injected paws 10.54 ± 10.06 %. Paw injection| time interaction analysis of variance measured by two-way ANOVA and Tukey's HSD correction for multiple comparisons p = 0.0018. m-IL-1α injected|un-injected p = 0.0075 (15 min) and m-IL-1α injected|un-injected (30 min) p = 0.0235. **c**. Mean ± SE paw withdrawal thresholds to mechanical stimuli before (0) and 15 and 30 mins after 20 µL injection of 5 µg/ml recombinant mouse IL-1α (m-IL-1α) in sterile PBS + 10% FBS (n = 6 mice). Mean ± SE for m-IL-1α: 3.58 ± 0.18 g and un-injected = 5.32 ± 0.52 g. **d.** Average percent change from baseline for each animal at indicated time points. Mean ± SE values at 15 min were m-IL-1a = -27.25 ± 2.22 % and un-injected = 3.78 ± 9.42 %. Paw injection| time interaction analysis of variance measured by two-way ANOVA and Tukey's HSD correction for multiple comparisons p = 0.0018. At 15 min m-IL-1α injected|un-injected p = 0.0205; 30 min m-IL-1α injected|un-injected p = 0.0068.

Figure 4. IL-1α reduces the optical rheobase of Trpv1/ChR2-EYFP mouse nociceptors. **a.** Representative Ca^{2+} transients evoked by various repetitive blue light stimulations (1, 5 and 10 pulses). Scale bars: 5 sec, 0.5 dF/F. **b.** Averaged percentage of sensory neurons activated by increasing pulses of blue light stimulations following treatment with vehicle and IL-1α (blue: 100 ng/ml IL-1α). Note that overnight incubation with IL-1α significantly increased the percentage of calcium-responsive cells compared to vehicle treatment ($F_{1,40}$ = 4.27; P = 0.045, two-way ANOVA with Bonferroni correction for multiple comparisons). All data represent mean

(point/line) ± SE (shaded area). **c.** Cumulative distributions of calcium response amplitudes measured in DRG somas in response to 100 ng/ml IL-1α (blue) or saline (grey).

Figure 5. Proposed mechanism for $Ca_V2.2$ channel involvement in inflammatory hypersensitivity. Capsaicin activates TRPV1 receptors on Trpv1-nociceptor nerve endings in skin, inducing a membrane depolarization that triggers the opening of voltage gated $Ca_V2.2$ channels. Calcium enters through both $Ca_V2.2$ channels and through Trpv1 channels, but the influx of calcium entry through $Ca_V2.2$ channels is critical for vesicular release of ATP from secretory vesicles. ATP binds to purinergic receptors expressed by keratinocytes and leukocytes to trigger release of IL-1α. IL-1α induces hypersensitivity of both heat nociceptors and mechanoreceptors.

Figure 1

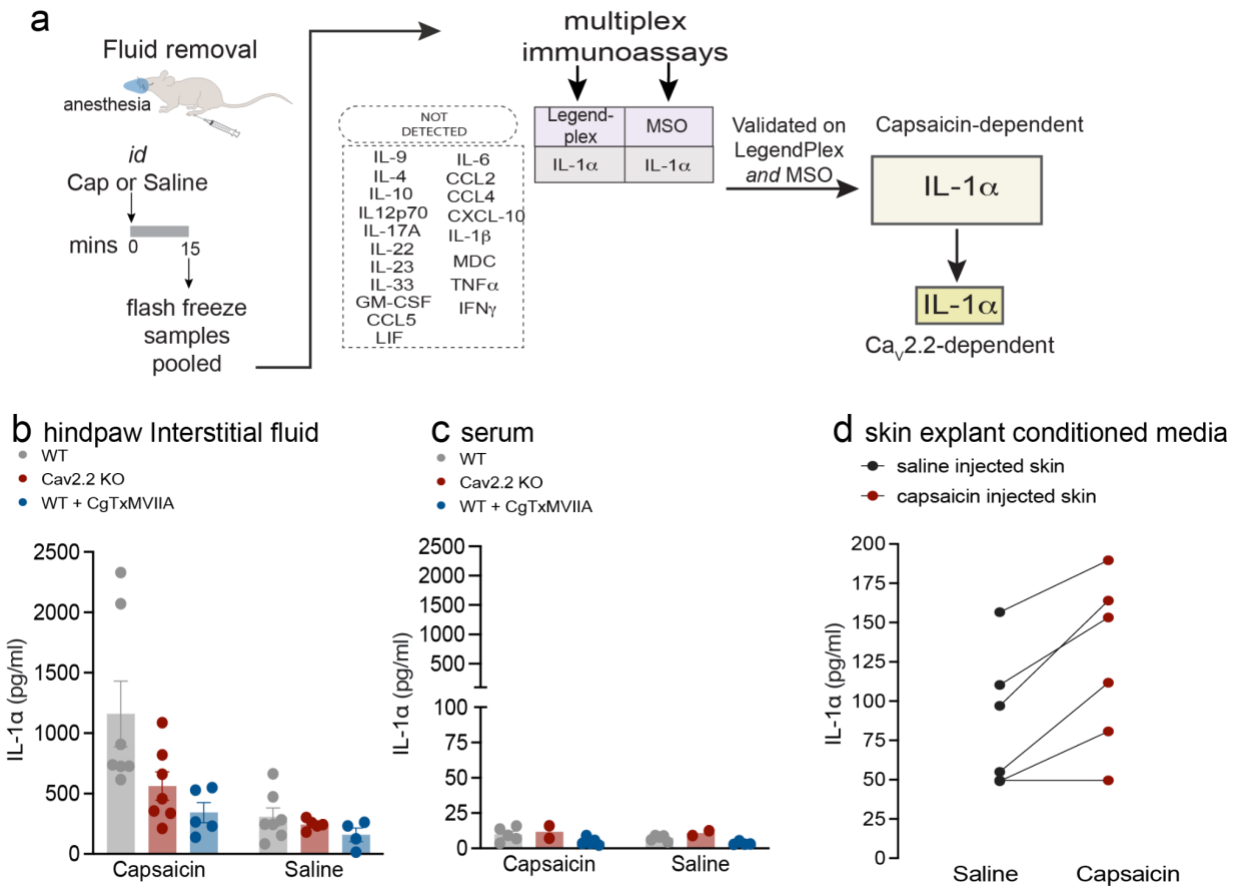
a
Fluid removal
anesthesia
id
Cap or Saline
mins 0
15
flash freeze
samples
pooled
multiplex
immunoassays
NOT DETECTED
IL-9
IL-4
IL-10
IL12p70
IL-17A
IL-22
IL-23
IL-33
GM-CSF
CCL5
LIF
IL-6
CCL2
CCL4
CXCL-10
IL-1β
MDC
TNFα
IFNγ
Legend-plex
MSO
IL-1α
IL-1α
Validated on LegendPlex and MSO
Capsaicin-dependent
IL-1α
IL-1α
Cav2.2-dependent
b hindpaw Interstitial fluid
WT
Cav2.2 KO
WT + CgTxMVIIA
IL-1α (pg/ml)
2500
2000
1500
1000
500
0
Capsaicin
Saline
c serum
WT
Cav2.2 KO
WT + CgTxMVIIA
IL-1α (pg/ml)
2500
2000
1500
1000
500
100
75
50
25
0
Capsaicin
Saline
d skin explant conditioned media
saline injected skin
capsaicin injected skin
IL-1α (pg/ml)
200
175
150
125
100
75
50
25
0
Saline
Capsaicin

Figure 2

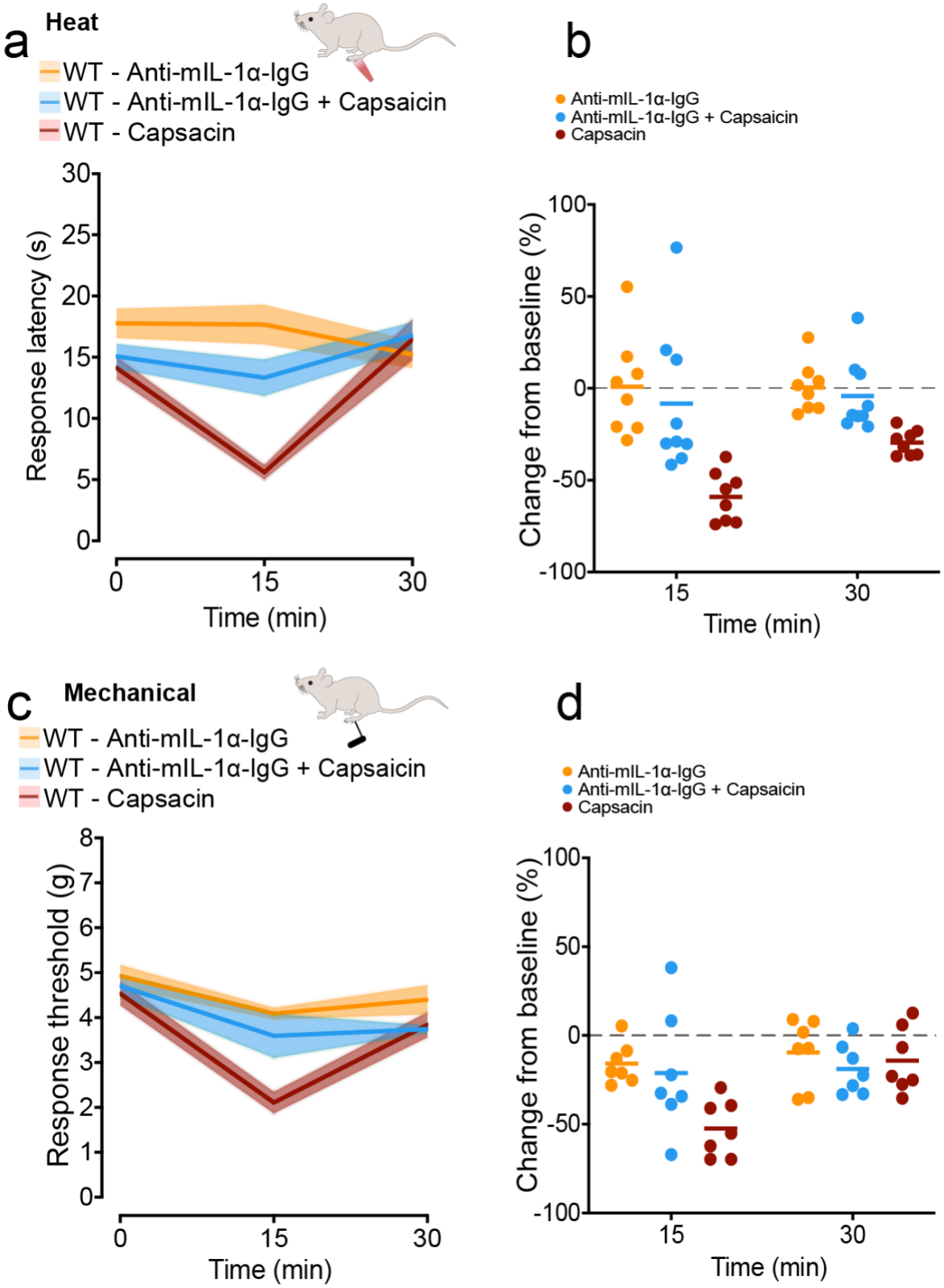
a
Heat
WT - Anti-mIL-1α-IgG
WT - Anti-mIL-1α-IgG + Capsaicin
WT - Capsacin
Response latency (s)
Time (min)
b
Anti-mIL-1α-IgG
Anti-mIL-1α-IgG + Capsaicin
Capsacin
Change from baseline (%)
Time (min)
c
Mechanical
WT - Anti-mIL-1α-IgG
WT - Anti-mIL-1α-IgG + Capsaicin
WT - Capsacin
Response threshold (g)
Time (min)
d
Anti-mIL-1α-IgG
Anti-mIL-1α-IgG + Capsaicin
Capsacin
Change from baseline (%)
Time (min)

Figure 3

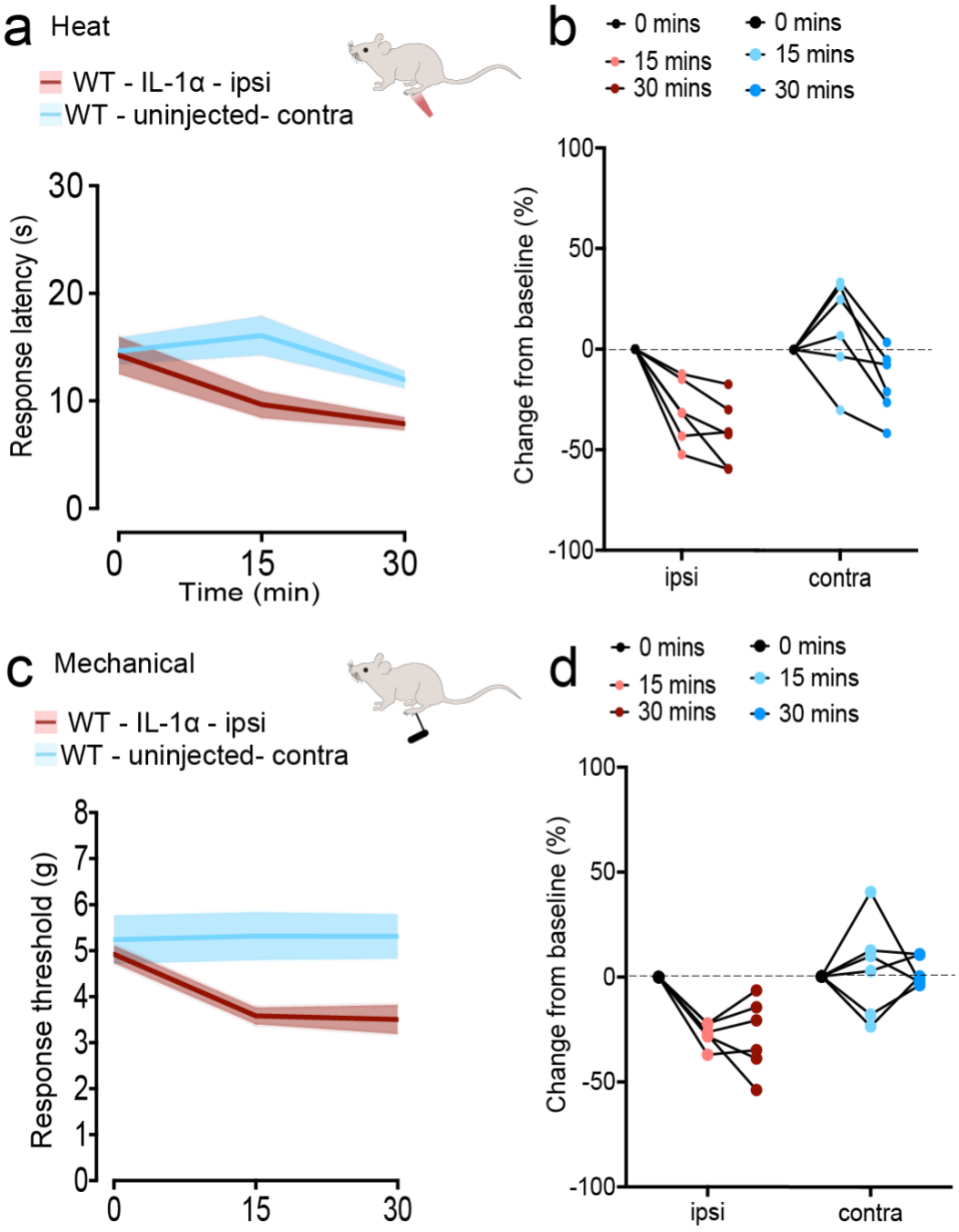
a
Heat
WT - IL-1α - ipsi
WT - uninjected- contra
Response latency (s)
30
20
10
0
0
15
30
Time (min)
b
0 mins
15 mins
30 mins
0 mins
15 mins
30 mins
Change from baseline (%)
100
50
0
-50
-100
ipsi
contra
c
Mechanical
WT - IL-1α - ipsi
WT - uninjected- contra
Response threshold (g)
8
7
6
5
4
3
2
1
0
0
15
30
d
0 mins
15 mins
30 mins
0 mins
15 mins
30 mins
Change from baseline (%)
100
50
0
-50
-100
ipsi
contra

Figure 4

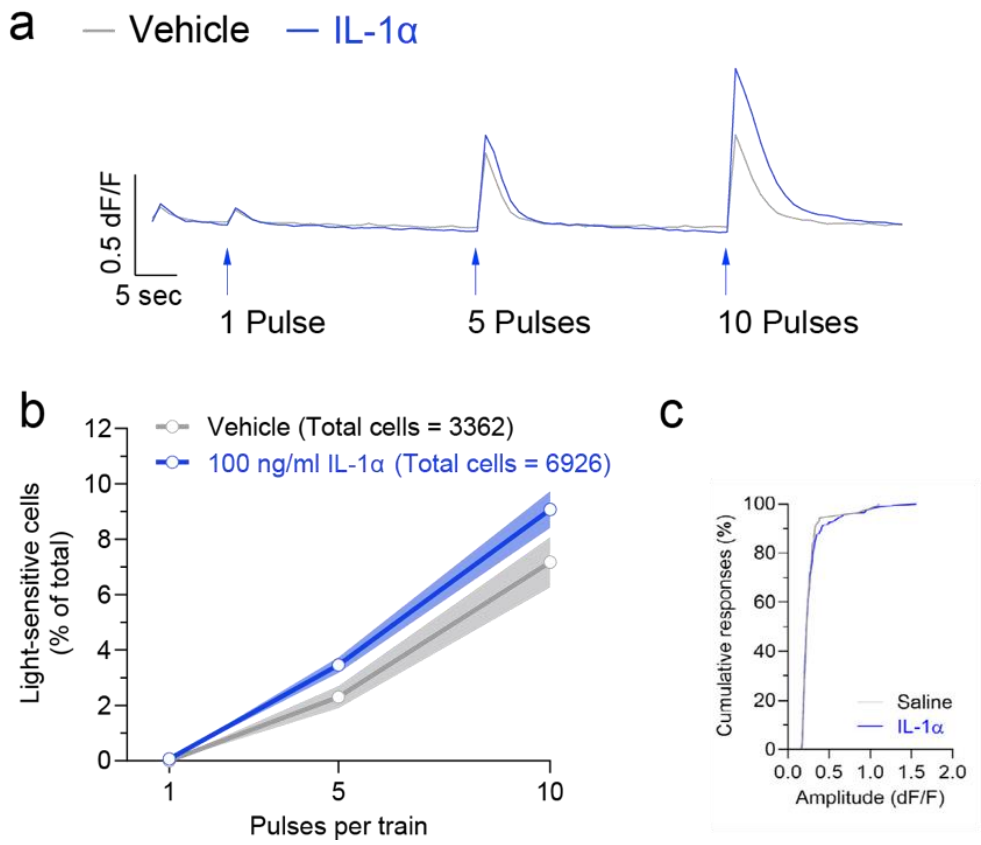
a
Vehicle
IL-1α
0.5 dF/F
5 sec
1 Pulse
5 Pulses
10 Pulses
b
Vehicle (Total cells = 3362)
100 ng/ml IL-1α (Total cells = 6926)
Light-sensitive cells (% of total)
Pulses per train
c
Cumulative responses (%)
Saline
IL-1α
Amplitude (dF/F)

Figure 5

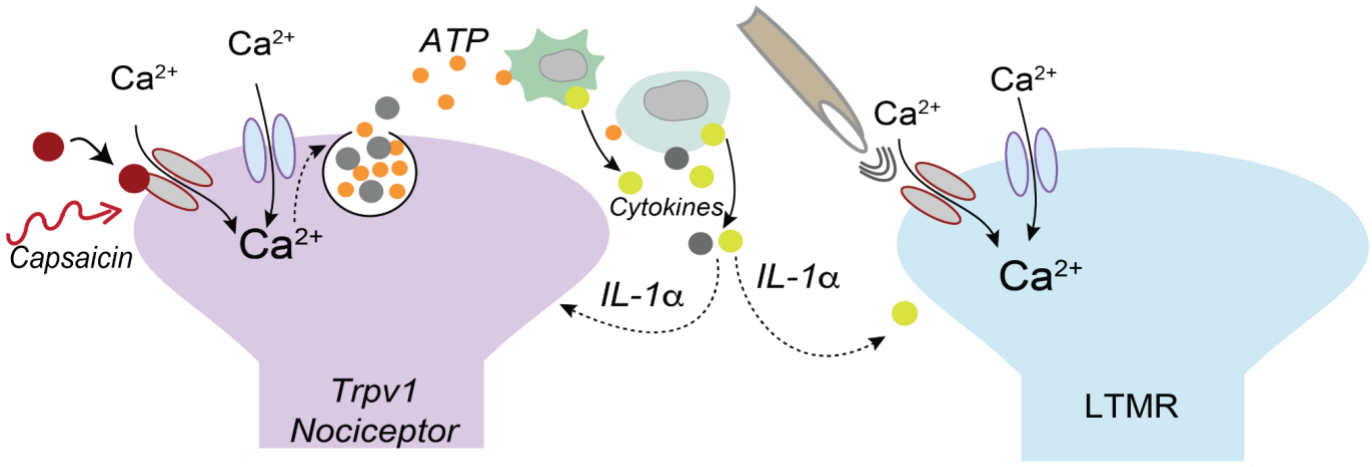
Ca2+
Ca2+
ATP
Ca2+
Ca2+
Capsaicin
Ca2+
Cytokines
IL-1α
IL-1α
Ca2+
Trpv1
Nociceptor
LTMR

1 Jain, A., Hakim, S. & Woolf, C. J. Unraveling the Plastic Peripheral Neuroimmune Interactome. *J Immunol* **204**, 257-263 (2020). https://doi.org/10.4049/jimmunol.1900818
2 Ji, R. R., Nackley, A., Huh, Y., Terrando, N. & Maixner, W. Neuroinflammation and Central Sensitization in Chronic and Widespread Pain. *Anesthesiology* **129**, 343-366 (2018). https://doi.org/10.1097/ALN.0000000000002130
3 Cook, S. P. & McCleskey, E. W. Cell damage excites nociceptors through release of cytosolic ATP. *Pain* **95**, 41-47 (2002). https://doi.org/10.1016/s0304-3959(01)00372-4
4 Costigan, M., Scholz, J. & Woolf, C. J. Neuropathic pain: a maladaptive response of the nervous system to damage. *Annu Rev Neurosci* **32**, 1-32 (2009). https://doi.org/10.1146/annurev.neuro.051508.135531
5 Scholz, J. & Woolf, C. J. Can we conquer pain? *Nat Neurosci* **5 Suppl**, 1062-1067 (2002).
6 Costigan, M. & Woolf, C. J. Pain: molecular mechanisms. *J Pain* **1**, 35-44 (2000).
7 Louis, S. M., Jamieson, A., Russell, N. J. & Dockray, G. J. The role of substance P and calcitonin gene-related peptide in neurogenic plasma extravasation and vasodilatation in the rat. *Neuroscience* **32**, 581-586 (1989). https://doi.org/10.1016/0306-4522(89)90281-9
8 DuBreuil, D. M. *et al.* Heat But Not Mechanical Hypersensitivity Depends on Voltage-Gated CaV2.2 Calcium Channel Activity in Peripheral Axon Terminals Innervating Skin. *J Neurosci* **41**, 7546-7560 (2021). https://doi.org/10.1523/JNEUROSCI.0195-21.2021
9 Giuliani, A. L., Sarti, A. C., Falzoni, S. & Di Virgilio, F. The P2X7 Receptor-Interleukin-1 Liaison. *Front Pharmacol* **8**, 123 (2017). https://doi.org/10.3389/fphar.2017.00123
10 Pinho-Ribeiro, F. A., Verri, W. A., Jr. & Chiu, I. M. Nociceptor Sensory Neuron-Immune Interactions in Pain and Inflammation. *Trends Immunol* **38**, 5-19 (2017). https://doi.org/10.1016/j.it.2016.10.001
11 Tamari, M., Ver Heul, A. M. & Kim, B. S. Immunosensation: Neuroimmune Cross Talk in the Skin. *Annu Rev Immunol* **39**, 369-393 (2021). https://doi.org/10.1146/annurev-immunol-101719-113805
12 Trier, A. M., Mack, M. R. & Kim, B. S. The Neuroimmune Axis in Skin Sensation, Inflammation, and Immunity. *J Immunol* **202**, 2829-2835 (2019). https://doi.org/10.4049/jimmunol.1801473
13 Binshtok, A. M. *et al.* Nociceptors are interleukin-1beta sensors. *J Neurosci* **28**, 14062-14073 (2008). https://doi.org/10.1523/JNEUROSCI.3795-08.2008
14 Summer, G. J. *et al.* Proinflammatory cytokines mediating burn-injury pain. *Pain* **135**, 98-107 (2008). https://doi.org/10.1016/j.pain.2007.05.012
15 Miller, R. J., Jung, H., Bhangoo, S. K. & White, F. A. Cytokine and chemokine regulation of sensory neuron function. *Handb Exp Pharmacol*, 417-449 (2009). https://doi.org/10.1007/978-3-540-79090-7_12
16 Baumann, T. K., Simone, D. A., Shain, C. N. & LaMotte, R. H. Neurogenic hyperalgesia: the search for the primary cutaneous afferent fibers that contribute to capsaicin-induced pain and hyperalgesia. *J Neurophysiol* **66**, 212-227 (1991). https://doi.org/10.1152/jn.1991.66.1.212
17 Gilchrist, H. D., Allard, B. L. & Simone, D. A. Enhanced withdrawal responses to heat and mechanical stimuli following intraplantar injection of capsaicin in rats. *Pain* **67**, 179-188 (1996). https://doi.org/10.1016/0304-3959(96)03104-1
18 Simone, D. A., Baumann, T. K. & LaMotte, R. H. Dose-dependent pain and mechanical hyperalgesia in humans after intradermal injection of capsaicin. *Pain* **38**, 99-107 (1989). https://doi.org/10.1016/0304-3959(89)90079-1
19 Bowersox, S., Mandema, J., Tarczy-Hornoch, K., Miljanich, G. & Luther, R. R. Pharmacokinetics of SNX-111, a selective N-type calcium channel blocker, in rats and cynomolgus monkeys. *Drug Metab Dispos* **25**, 379-383 (1997).

20 Wang, Y. X. *et al.* Peripheral versus central potencies of N-type voltage-sensitive calcium channel blockers. *Naunyn Schmiedebergs Arch Pharmacol* **357**, 159-168 (1998). https://doi.org/10.1007/pl00005150
21 White, D. M. & Cousins, M. J. Effect of subcutaneous administration of calcium channel blockers on nerve injury-induced hyperalgesia. *Brain Res* **801**, 50-58 (1998). https://doi.org/10.1016/s0006-8993(98)00539-3
22 Xiao, W. H. & Bennett, G. J. Synthetic omega-conopeptides applied to the site of nerve injury suppress neuropathic pains in rats. *J Pharmacol Exp Ther* **274**, 666-672 (1995).
23 DuBreuil, D. M. *et al.* A high-content platform for physiological profiling and unbiased classification of individual neurons. *Cell Rep Methods* **1** (2021). https://doi.org/10.1016/j.crmeth.2021.100004
24 Sandkuhler, J. Models and mechanisms of hyperalgesia and allodynia. *Physiol Rev* **89**, 707-758 (2009). https://doi.org/10.1152/physrev.00025.2008
25 Liu, M., Max, M. B., Robinovitz, E., Gracely, R. H. & Bennett, G. J. The human capsaicin model of allodynia and hyperalgesia: sources of variability and methods for reduction. *J Pain Symptom Manage* **16**, 10-20 (1998). https://doi.org/10.1016/s0885-3924(98)00026-8
26 Stenina, M. A. *et al.* Cytokine profile of the blood in mice with normal and abnormal heart rhythm. *Bull Exp Biol Med* **152**, 692-695 (2012). https://doi.org/10.1007/s10517-012-1608-9
27 Rider, P., Voronov, E., Dinarello, C. A., Apte, R. N. & Cohen, I. Alarmins: Feel the Stress. *J Immunol* **198**, 1395-1402 (2017). https://doi.org/10.4049/jimmunol.1601342
28 Li, Y. *et al.* Cytokine patterns in the blister fluid and plasma of patients with fracture blisters. *Int Immunopharmacol* **123**, 110738 (2023). https://doi.org/10.1016/j.intimp.2023.110738
29 Sjobom, U., Christenson, K., Hellstrom, A. & Nilsson, A. K. Inflammatory Markers in Suction Blister Fluid: A Comparative Study Between Interstitial Fluid and Plasma. *Front Immunol* **11**, 597632 (2020). https://doi.org/10.3389/fimmu.2020.597632
30 Cavalli, G. *et al.* Interleukin 1alpha: a comprehensive review on the role of IL-1alpha in the pathogenesis and treatment of autoimmune and inflammatory diseases. *Autoimmun Rev* **20**, 102763 (2021). https://doi.org/10.1016/j.autrev.2021.102763
31 Werman, A. *et al.* The precursor form of IL-1alpha is an intracrine proinflammatory activator of transcription. *Proc Natl Acad Sci U S A* **101**, 2434-2439 (2004). https://doi.org/10.1073/pnas.0308705101
32 Dinarello, C. A. Overview of the IL-1 family in innate inflammation and acquired immunity. *Immunol Rev* **281**, 8-27 (2018). https://doi.org/10.1111/imr.12621
33 Lonnemann, G. *et al.* Differences in the synthesis and kinetics of release of interleukin 1 alpha, interleukin 1 beta and tumor necrosis factor from human mononuclear cells. *Eur J Immunol* **19**, 1531-1536 (1989). https://doi.org/10.1002/eji.1830190903
34 Mantovani, A., Dinarello, C. A., Molgora, M. & Garlanda, C. Interleukin-1 and Related Cytokines in the Regulation of Inflammation and Immunity. *Immunity* **50**, 778-795 (2019). https://doi.org/10.1016/j.immuni.2019.03.012
35 Martin, P., Goldstein, J. D., Mermoud, L., Diaz-Barreiro, A. & Palmer, G. IL-1 Family Antagonists in Mouse and Human Skin Inflammation. *Front Immunol* **12**, 652846 (2021). https://doi.org/10.3389/fimmu.2021.652846
36 Hung, A. L., Lim, M. & Doshi, T. L. Targeting cytokines for treatment of neuropathic pain. *Scand J Pain* **17**, 287-293 (2017). https://doi.org/10.1016/j.sjpain.2017.08.002
37 Vanderwall, A. G. & Milligan, E. D. Cytokines in Pain: Harnessing Endogenous Anti-Inflammatory Signaling for Improved Pain Management. *Front Immunol* **10**, 3009 (2019). https://doi.org/10.3389/fimmu.2019.03009

38 Scholz, J. & Woolf, C. J. The neuropathic pain triad: neurons, immune cells and glia. *Nat Neurosci* **10**, 1361-1368 (2007). https://doi.org/10.1038/nn1992
39 Huntula, S., Saegusa, H., Wang, X., Zong, S. & Tanabe, T. Involvement of N-type Ca(2+) channel in microglial activation and its implications to aging-induced exaggerated cytokine response. *Cell Calcium* **82**, 102059 (2019). https://doi.org/10.1016/j.ceca.2019.102059
40 Saegusa, H. *et al.* Suppression of inflammatory and neuropathic pain symptoms in mice lacking the N-type Ca2+ channel. *EMBO J* **20**, 2349-2356 (2001). https://doi.org/10.1093/emboj/20.10.2349
41 Sharma, N. *et al.* The emergence of transcriptional identity in somatosensory neurons. *Nature* **577**, 392-398 (2020). https://doi.org/10.1038/s41586-019-1900-1
42 Cai, S., Gomez, K., Moutal, A. & Khanna, R. Targeting T-type/CaV3.2 channels for chronic pain. *Transl Res* **234**, 20-30 (2021). https://doi.org/10.1016/j.trsl.2021.01.002
43 Stemkowski, P. L. *et al.* Identification of interleukin-1 beta as a key mediator in the upregulation of Cav3.2-USP5 interactions in the pain pathway. *Mol Pain* **13**, 1744806917724698 (2017). https://doi.org/10.1177/1744806917724698
44 Picard, E. *et al.* Role of T CD4(+) cells, macrophages, C-low threshold mechanoreceptors and spinal Ca(v) 3.2 channels in inflammation and related pain-like symptoms in murine inflammatory models. *Br J Pharmacol* **180**, 385-400 (2023). https://doi.org/10.1111/bph.15956
45 Culp, W. J., Ochoa, J., Cline, M. & Dotson, R. Heat and mechanical hyperalgesia induced by capsaicin. Cross modality threshold modulation in human C nociceptors. *Brain* **112 (Pt 5)**, 1317-1331 (1989). https://doi.org/10.1093/brain/112.5.1317
46 Magerl, W., Fuchs, P. N., Meyer, R. A. & Treede, R. D. Roles of capsaicin-insensitive nociceptors in cutaneous pain and secondary hyperalgesia. *Brain* **124**, 1754-1764 (2001). https://doi.org/10.1093/brain/124.9.1754
47 Szolcsanyi, J., Anton, F., Reeh, P. W. & Handwerker, H. O. Selective excitation by capsaicin of mechano-heat sensitive nociceptors in rat skin. *Brain Res* **446**, 262-268 (1988). https://doi.org/10.1016/0006-8993(88)90885-2
48 Koltzenburg, M., Stucky, C. L. & Lewin, G. R. Receptive properties of mouse sensory neurons innervating hairy skin. *J Neurophysiol* **78**, 1841-1850 (1997). https://doi.org/10.1152/jn.1997.78.4.1841
49 Stemkowski, P. L., Noh, M. C., Chen, Y. & Smith, P. A. Increased excitability of medium-sized dorsal root ganglion neurons by prolonged interleukin-1beta exposure is K(+) channel dependent and reversible. *J Physiol* **593**, 3739-3755 (2015). https://doi.org/10.1113/JP270905
50 Stemkowski, P. L. & Smith, P. A. Long-term IL-1beta exposure causes subpopulation-dependent alterations in rat dorsal root ganglion neuron excitability. *J Neurophysiol* **107**, 1586-1597 (2012). https://doi.org/10.1152/jn.00587.2011
51 von Banchet, G. S. *et al.* Molecular effects of interleukin-1beta on dorsal root ganglion neurons: prevention of ligand-induced internalization of the bradykinin 2 receptor and downregulation of G protein-coupled receptor kinase 2. *Mol Cell Neurosci* **46**, 262-271 (2011). https://doi.org/10.1016/j.mcn.2010.09.009
52 Prado, J. *et al.* Cytokine receptor clustering in sensory neurons with an engineered cytokine fusion protein triggers unique pain resolution pathways. *Proc Natl Acad Sci U S A* **118** (2021). https://doi.org/10.1073/pnas.2009647118
53 Beaudry, H., Daou, I., Ase, A. R., Ribeiro-da-Silva, A. & Seguela, P. Distinct behavioral responses evoked by selective optogenetic stimulation of the major TRPV1+ and MrgD+ subsets of C-fibers. *Pain* **158**, 2329-2339 (2017). https://doi.org/10.1097/j.pain.0000000000001016

54 Li, L. *et al.* The functional organization of cutaneous low-threshold mechanosensory neurons. *Cell* **147**, 1615-1627 (2011). https://doi.org/10.1016/j.cell.2011.11.027

55 Barabas, M. E. & Stucky, C. L. TRPV1, but not TRPA1, in primary sensory neurons contributes to cutaneous incision-mediated hypersensitivity. *Mol Pain* **9**, 9 (2013). https://doi.org/10.1186/1744-8069-9-9

56 Hargreaves, K., Dubner, R., Brown, F., Flores, C. & Joris, J. A new and sensitive method for measuring thermal nociception in cutaneous hyperalgesia. *Pain* **32**, 77-88 (1988). https://doi.org/10.1016/0304-3959(88)90026-7